Characterization of a Glycidyl Azide Polymer Composite Propellant: Strain Rate Effects and Relaxation Response

E. J. S. DUNCAN

Defence Research Establishment Valcartier, Courcelette, Québec, Canada G0A 1R0

SYNOPSIS

Uniaxial tension tests were completed on a developmental GAP/PSAN solid rocket propellant at constant strain rates ranging over three decades and at five different temperatures. An analysis of the maximum stress (strength) and the strain at maximum stress showed that there is a relatively narrow range of temperatures and strain rates that give rise to strains at maximum stress that exceed 18%. The long-term equilibrium strain capability (strain endurance) appears to be between 10% and 12%. The trend of the strength and initial deformation moduli were log-linear with the reciprocal of the strain rate across three decades. However, the shifted master curves were log-curvilinear in form. The relationship between the strength and the initial modulus can be approximated by a power law. A series of stress relaxation tests was completed at a level of 4% strain and at five different temperatures. The initial portion of the shifted master relaxation curve is concave-up with correspondingly high stresses and moduli. It decays with time approaching a log-constant slope. Tensile moduli derived from constant strain rate tests were found to be consistently higher in value than the moduli as a function of time determined from relaxation tests, for an equivalent shifted time. Preliminary evidence suggests that the tensile modulus as a function of the reciprocal of shifted strain rate can be equated to the relaxation modulus as a function of shifted time through an adjustment factor. This relationship extends the relaxation modulus results back a further three and one-half decades of shifted time.

INTRODUCTION

The Defence Research Establishment Valcartier (DREV) has developed a new insensitive smokeless solid rocket propellant based on energetic glycidyl azide polymer (GAP) and phase stabilized ammonium nitrate (PSAN) as the oxidiser.[1] Characterization of the mechanical properties of a solid rocket propellant is fundamental to determining whether the loaded polymer is capable of maintaining certain dimensional stability and structural integrity over a wide variety of environmental storage conditions as well as aerodynamic thermal and inertial loads.

The results presented in this paper document some of the work that has taken place concerning the ultimate failure properties of GAP/PSAN and the effect that constant strain rates have on these properties, as well as the nature of the time-dependent relaxation response. It was also determined that an equivalency exists between constant strain rate tests and time-dependent relaxation tests based on time–temperature superposition theory.

Journal of Applied Polymer Science, Vol. 56, 365–375 (1995)
 CCC 0021-8995/95/030365-11

EXPERIMENTAL PROCEDURE

All tests were completed in uniaxial tension. Specimens for the constant strain rate/temperature tests were from batch 2946 (with the exception of the tests at 0°C, which came from batch 2947). Specimens for the relaxation tests were from batch 2957 (with the exception of the tests at 0°C, which came from batch 2947).

Constant Strain Rate/Temperature Tests

Uniaxial tension tests were completed at four strain rates ranging over three decades of magnitude and

at five different temperatures according to the test matrix presented in Table I. Four specimens were tested at each strain rate and temperature.

Test Specimens and Procedures

Standard JANNAF (Joint Army–Navy–NASA–Air Force) Class C "dog-bone" test specimens were used in all constant strain rate uniaxial tension tests in this study.[2] Each specimen was punched from a precast 12.7 mm ($\frac{1}{2}$ in) thick slab of GAP/PSAN propellant using a hydraulic press and die. The specimen cross-section was determined from the average of three measurements of the width and thickness along the length of the narrow portion of the specimen. The effective gauge length for the JANNAF dog-bone specimen was determined using a laser extensometer and found to be 86.49 mm at a strain rate of 0.58 min^{-1} and a temperature of 23°C. This constant value was used for all tests. The strain was calculated by dividing the change in the displacement by the effective gauge length.

Tensile testing was completed on an Instron Model 1122 with a temperature box and controller. All specimens were preconditioned at the test temperature for approximately 1 h prior to testing.

Instron Series IX software was used for data acquisition and data reduction. The tensile modulus for materials that characteristically respond with a low stress, concave-up region during the early stages of a test, such as filled composite propellants, was determined by computing a "least squares fit" straight line through consecutive segments of data, beginning at the start of the test and progressing along the curve up to the maximum stress. The highest slope measured was defined as the tensile modulus.

Time-Dependent Relaxation Tests

Time-dependent relaxation tests were completed at five temperatures (−30, −17.5, 0, 20, and 40°C) and a fixed strain level of 4%. Each specimen was placed in a latex rubber sheath with desiccant to ensure strict humidity control. Three specimens were tested at each temperature; not every test result was available at each temperature, however, because in some instances the specimen debonded during testing. The exception to the above is the test at 0°C, which involved only one specimen and did not use desiccant. The tests ranged in duration from 3.5 h to 3 days, with the test at −30°C being the longest.

Test Specimens and Procedures

The samples used for the stress relaxation tests were punched from a 12.7 mm ($\frac{1}{2}$ in) thick precast slab of GAP/PSAN propellant using a hydraulic press and a die. Samples were rectangular in shape, measuring 127 mm in length and approximately 11.8 mm in width. The specimen cross-section was determined from the average of three measurements of the width and thickness along the length of the specimen. Phenolic/pine tabs 12.7 × 12.7 × 20 mm in length were bonded to the end of each specimen. The tab-bonded test specimen was secured by means of a steel pin through a hole in the tab to a U-shaped grip and tie-rod assembly inside a multi-specimen loading frame. Temperature control was provided by a Webber temperature conditioning chamber. The load frame uses a spring driven loading assembly to apply a fixed displacement to each specimen. The corresponding strain on each specimen was calculated by dividing the displacement by the gauge length, which in this case was the original length of the specimen. Individual load cells measured the decay in the force with time for each specimen. All specimens were preconditioned at the test temperature for approximately 1 h prior to testing.

When reducing the stress relaxation test data, time zero was considered to have commenced when the stress reached its highest value during the application of the fixed displacement. The initial transient effects in the relaxation response were omitted

Table I Constant Strain Rate Uniaxial Tension Test Matrix

		Temperature °C				
Disp Rate (mm/min)	Strain Rate (min^{-1})	−40	−30	0*	20	60
0.5	0.0058	x	x	x	x	x
5.0	0.0578	x	x	x	x	x
50	0.5779	x	x	x	x	x
500	5.78	x	x	x	x	x

* Tests completed on batch 2947; other temperatures on batch 2946.

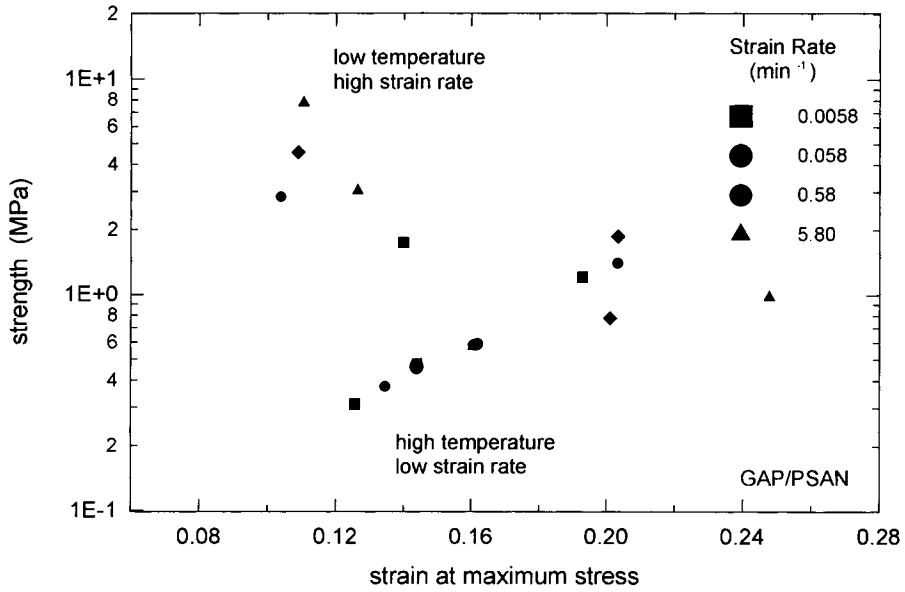

Figure 1 Stress–strain failure boundary plot for uniaxial tension tests on GAP/PSAN.

in all figures in this paper unless noted otherwise. To determine the transient portion, the time taken to reach the peak stress was multiplied by 10 and this length of time was then omitted from the first part of the results.

RESULTS AND DISCUSSION

The range of temperatures investigated in this study covers the accepted range of temperatures for GAP/PSAN in expected service-life scenarios. Constant strain rate testing was limited to a three decade range of magnitude, where it was anticipated that it would be possible to undertake a comparative study of the equivalency between loading rate and time-dependent effects. Additional testing at both lower and faster rates is planned based on the results of this study.

Temperature and Rate Dependence of Mechanical Properties

All testing was completed on uniaxial specimens at nominally constant strain rates up to failure. The mechanical properties that were measured included the strain at maximum stress, maximum stress (strength), and tensile modulus.

The relationship between strength and strain at maximum stress is shown in Figure 1. This is often referred to as a Smith failure envelope plot.[3] Theoretically, the Smith failure envelope is based on the premise that the failure boundary is path-independent. This implies that failure points would lie on the same boundary whether the path to failure was a constant strain rate, constant stress rate, or any other stress–strain path. Research by others has shown that this is not always valid for loaded propellants.[4,5] Until it can be demonstrated that failure is path-independent for GAP/PSAN propellant, a plot such as that shown in Figure 1 will be considered merely a convenient method of presenting constant strain-rate data.

Two things are immediately apparent from the stress–strain failure boundary plot. First, there is a limited range of temperatures for any given strain rate where the measured strain at maximum stress exceeded 17%. Strains at maximum stress in excess of 17% were measured at −30°C at the two lowest strain rates of 0.0058 and 0.058 min^{-1}. At 0.58 min^{-1}, strains at maximum stress in excess of 17% were measured at temperatures of −30, 0, and 23°C, while at 5.8 min^{-1} strains at maximum stress in excess of 17% were measured only at temperatures of 0 and 23°C. The highest strain of 24.8% was measured at 23°C at a strain rate of 5.8 min^{-1}. Second, the trend of the stress–strain data in the high temperature/low strain rate region of the curve suggests that the long-term equilibrium strain capability (strain endurance) of GAP/PSAN propellant is between 10% and 12%.

Figure 2 is a plot of the tensile modulus versus the reciprocal of the strain rate, in log space, for five different temperatures. Results at 0°C were included

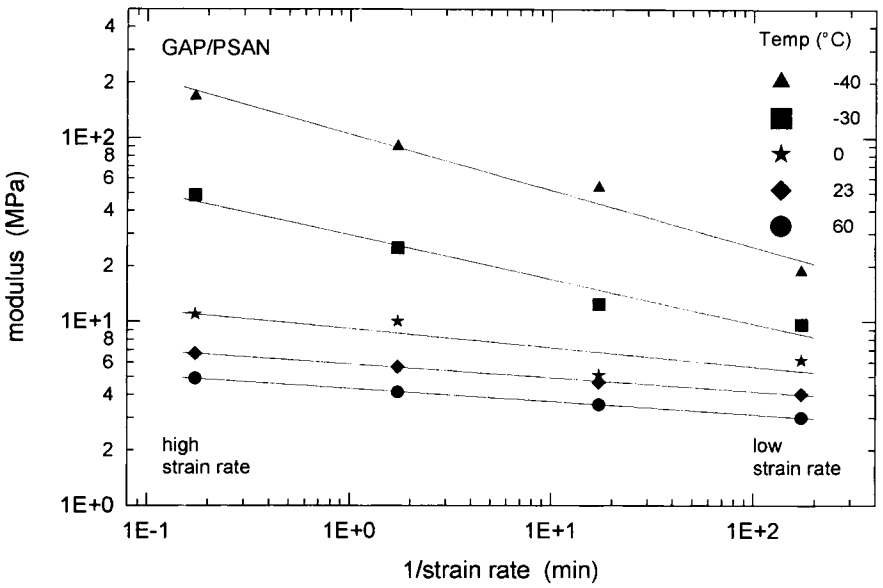

Figure 2 Uniaxial tension tests on GAP/PSAN showing the tensile modulus versus the reciprocal of the constant strain rate.

in Figure 2 from a series of tests on specimens from batch 2947. Two features characterize this plot. The first is the log-linearity of the data across three decades of strain rates at all temperatures. Second, the slope of the data did not remain the same over the entire temperature range investigated. Two distinct slopes are apparent, one common to the data at 60, 23, and 0°C, and a higher slope common to the data at −30 and −40°C. The effect that strain rate has on the tensile modulus at discrete temperatures is illustrated in Figure 3, a plot of the tensile modulus versus temperature. The most probable reason for the dramatic increase in the stiffness at lower temperatures as the strain rate increases is a reduction in the molecular mobility of the glycidyl azide polymer chains as the glass transition temperature is approached.

Figure 4 shows a plot of the strength versus the

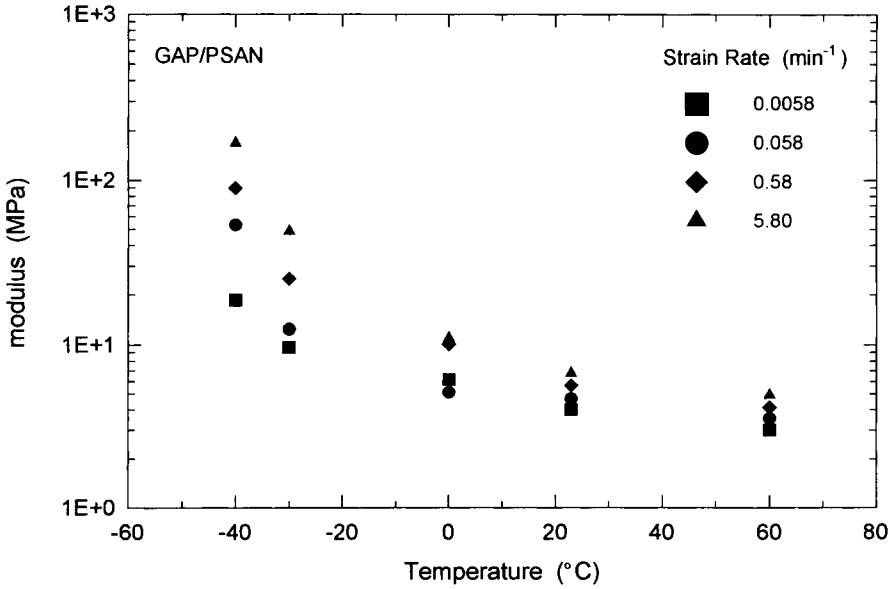

Figure 3 Uniaxial tension tests on GAP/PSAN showing the tensile modulus versus the temperature at various strain rates.

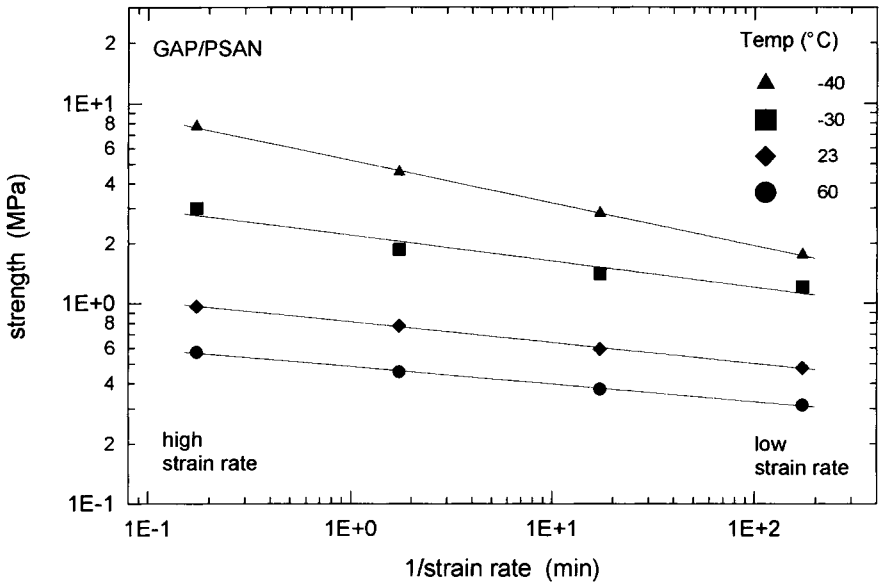

Figure 4 Uniaxial tension tests on GAP/PSAN showing the strength versus the reciprocal of the constant strain rate.

reciprocal of the strain rate, in log space, for four different temperatures. Data points for the results at 0°C were not plotted because the strengths were consistently low. The strength data is similar to the tensile modulus data in that it remained log-linear across three decades of strain rates at all temperatures. The notable increase in the slope occurs at −40°C rather than at −30°C, as was the case for the tensile modulus data, suggesting that the strength of GAP/PSAN is less affected by changes in the molecular mobility of the network polymer chains as the glass transition is approached.

The relationship between the strength and the tensile modulus is shown in Figure 5. The symbols represent tests at different temperatures where the strain rate increases up the curve within each temperature range. A power law function of the form

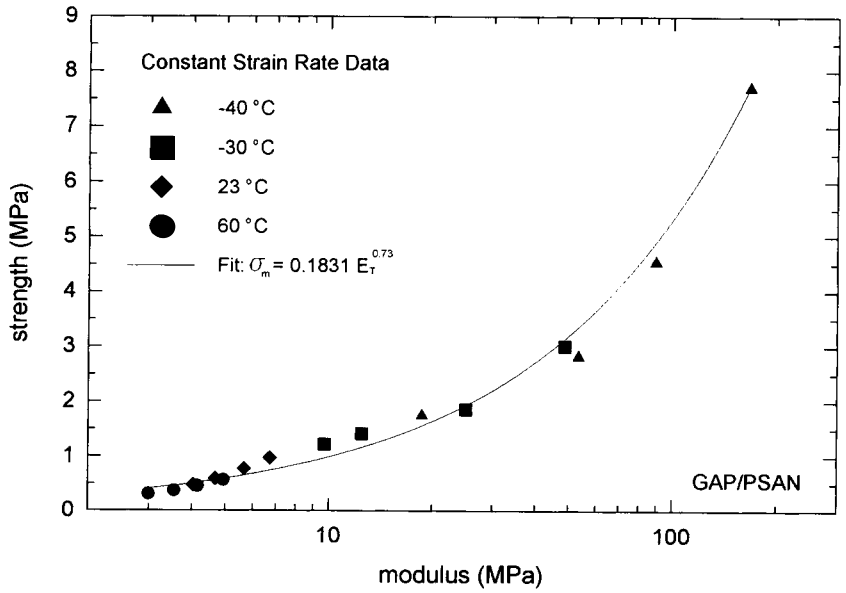

Figure 5 Strength versus the tensile modulus for GAP/PSAN. Solid line is a power law fit.

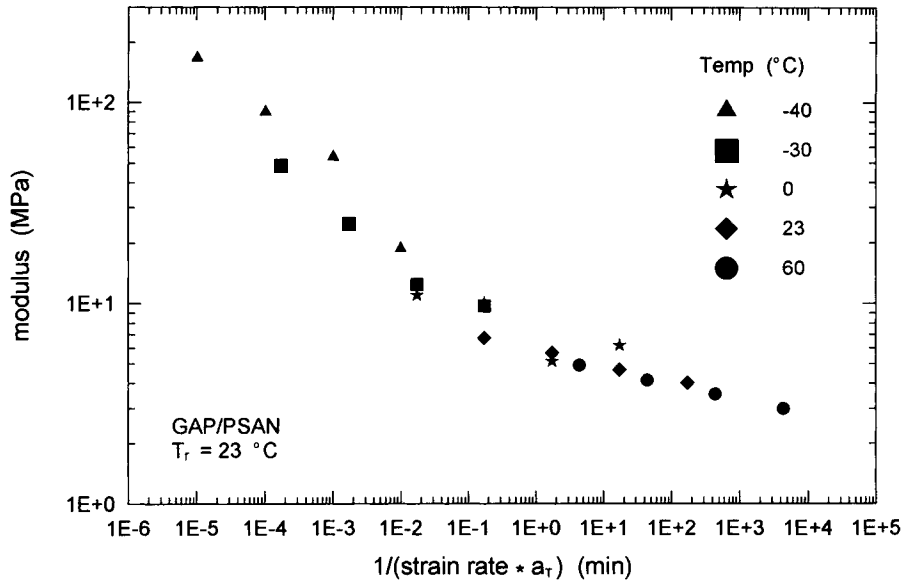

Figure 6 Shifted master curve of the tensile modulus for GAP/PSAN.

$$\sigma_m = AE_T^n \tag{1}$$

was determined to best describe the data. σ_m is the strength, E_T is the tensile modulus, A is a constant having a value of 0.1831, and n is the modulus exponent, which has a value of 0.73. Although such a relationship is not often addressed in the literature, it does demonstrate that there is a trend toward a long-term "limit" strength and modulus.

Because of the viscoelastic nature of composite solid propellants, the failure strength and tensile modulus, as well as the strain at maximum stress, are time- and temperature-dependent. As a result they can be superposed into master curves using time-temperature equivalency principles.[6] Data in this study (unless otherwise noted) were shifted to master curves using the Williams–Landel–Ferry (WLF) equation

$$\log a_T = \frac{-C_1(T - T_r)}{C_2 + T - T_r}, \tag{2}$$

where a_T is the shift factor, C_1 and C_2 are "best-fit" constants, T is the temperature of the test data, and T_r is the reference temperature. The shifted master tensile modulus curve is shown in Figure 6. It has a well defined concave-up, curvilinear form. The shift factors (a_T) used to shift the tensile modulus data at each temperature are given in Table II. The shifted master uniaxial strength curve has the same general appearance (Fig. 7), although the curvilinear nature of the master curve is less pronounced. Values for a_T at each temperature are given in Table II.

The results of the time-temperature shift of the strain at maximum stress are shown in Figure 8. The shifted curve was constructed from shift factors measured directly from the data. A characteristic "straw hat" shape is evident. High temperatures and low

Table II Shift Factors for the Results of the Constant Strain Rate Tests

Temperature (°C)	Tensile Modulus Shift Factor a_T	Uniaxial Strength Shift Factor a_T	Strain at Maximum Stress Shift Factor a_T
60	0.04	0.003	0.01
23	1.0	1.0	1.0
0	10.0	—	—
−30	996.0	3711.0	32.0
−40	16991.0	440647.0	22060.0

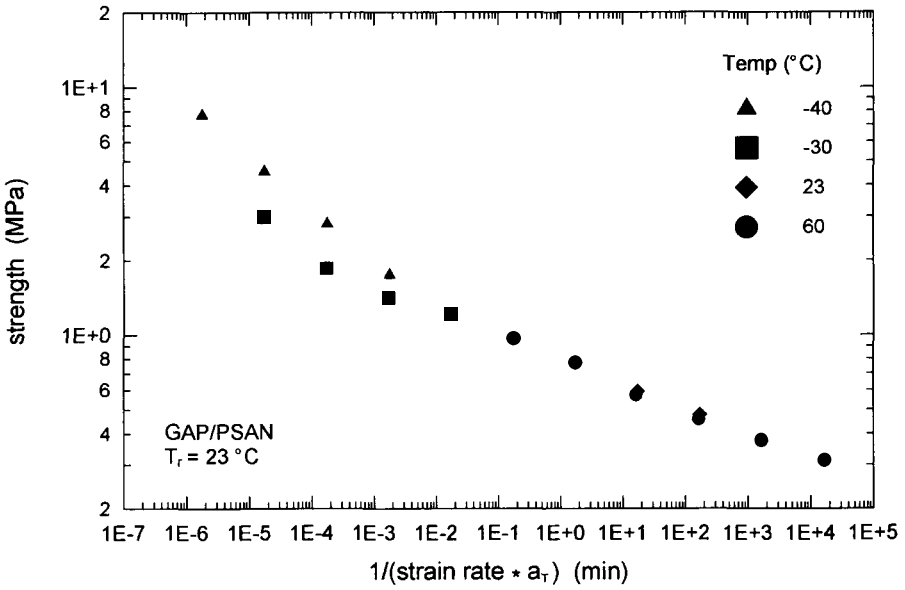

Figure 7 Shifted master curve of the uniaxial tensile strength for GAP/PSAN.

strain rates are found on the extreme right of the master curve. The trend at this location suggests that the long-term equilibrium strain capability (strain endurance) is between 10% and 12%. This corroborates the results suggested by Figure 1. Values for a_T at each temperature are given in Table II.

Time-Dependent Relaxation Tests

Relaxation tests were completed at a strain level of 4% at five temperatures (−30, −17, 0, 20, and 40°C). The results of the relaxation tests are presented in Figure 9. In general, the relaxation responses at 0, −17, and −30°C are characterized by a distinct concave-up form that appears to ultimately resolve into a log-constant rate of decay with approximately the same slope as the relaxation responses at 20 and 40°C. The lower the temperature, the later this transition occurs. Between 0 and 20°C the transition is lost in the transient effects, due to loading. When the relaxation responses are shifted to a master curve, the result is a curvilinear (concave-up) master

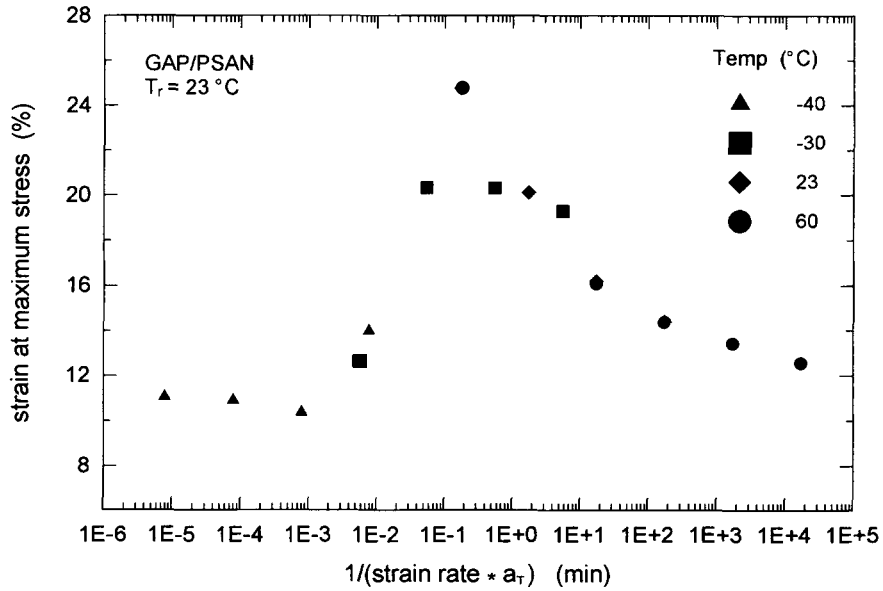

Figure 8 Shifted master curve of the strain at peak stress for GAP/PSAN.

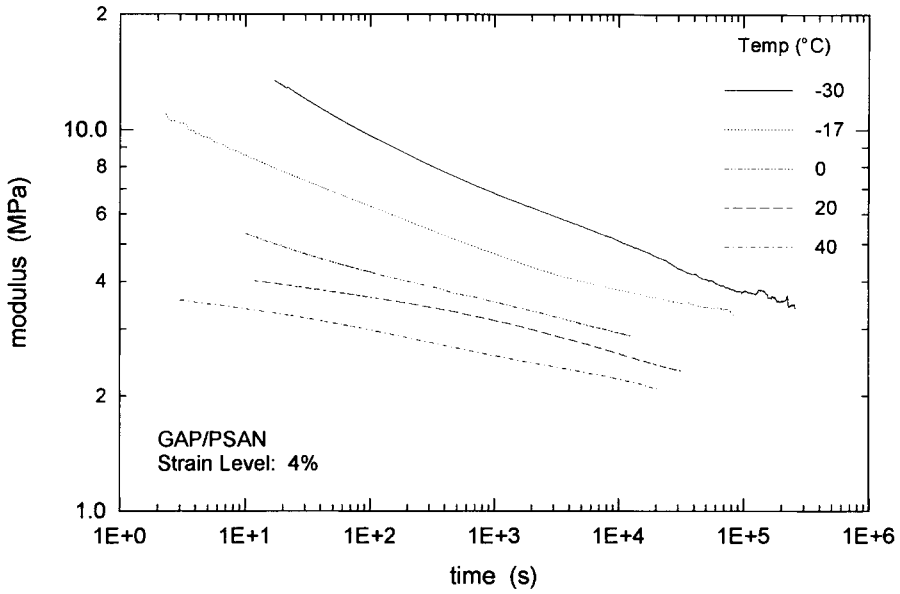

Figure 9 Modulus relaxation curves for GAP/PSAN solid propellant.

relaxation response (Fig. 10). The modulus relaxation curve was derived directly from stress relaxation data by dividing the measured stress by the applied strain. It is characterized by the same curvilinear form as the shifted master tensile modulus and shifted master strength curves discussed earlier. Values for a_T at each temperature are given in Table III.

It should be noted that the shift factors determined for the three mechanical properties obtained from constant strain tests varied considerably. Ideally, a_T should be the same function of temperature if a material behaves linear-viscoelastically over its entire range of response up to failure. Highly filled elastomers are known to exhibit nonlinear behavior at relatively small deformations.[7,8] It is not surprising then, that the a_T values for the strength and strain at maximum stress agree less well with the values for the tensile modulus and the relaxation modulus. The former two mechanical properties occur well outside the linear viscoelastic zone of a filled elastomer propellant. As Figure 11 illustrates, shift

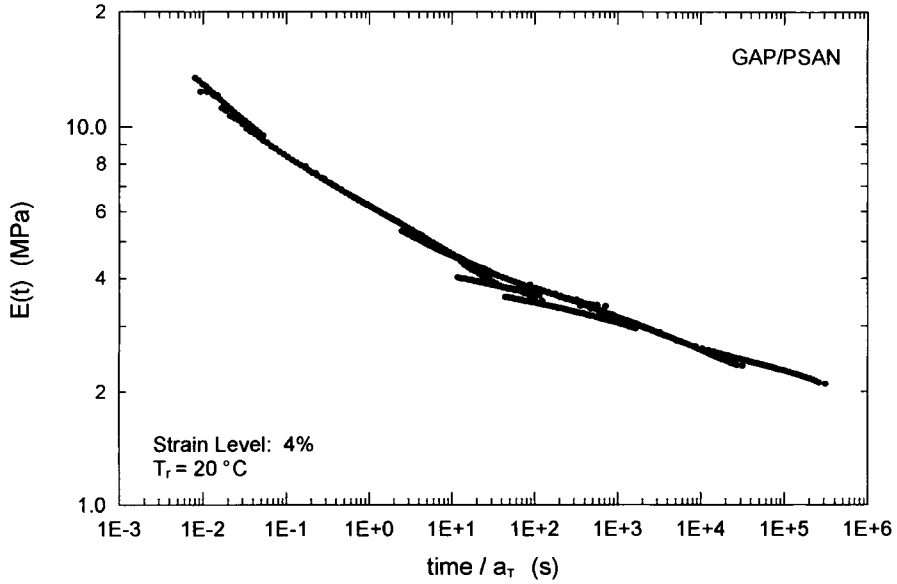

Figure 10 Master modulus relaxation curve for GAP/PSAN solid propellant.

Table III Shift Factors for Master Modulus Relaxation Curve

Temperature (°C)	Shift Factor a_T
40	0.07
20	1.0
0	4.0
−17	115.0
−30	2085.0

factors for the tensile modulus data derived from the constant strain rate tests and those for the modulus as a function of time determined from the relaxation tests were found to be in reasonable agreement. A three-parameter function that best describes this relationship is also shown.

Since the reciprocal of strain rate has units of time, it is possible to compare the shifted master tensile modulus data obtained from constant strain rate tests (Fig. 6) and the shifted master modulus relaxation data obtained from relaxation tests (Fig. 10). The results of this comparison are shown in Figure 12. It can be seen that the tensile moduli are higher in value than the relaxation moduli for any equivalent shifted time. Although there is not a direct correspondence between relaxation time and the reciprocal of strain rate, where the two master curves overlap they show a remarkably similar trend and slope. This relationship is sufficient to suggest that the tensile modulus as a function of the reciprocal of shifted strain rate may be equated to the relaxation modulus as a function of shifted time through an adjustment factor, here defined as A_f. This is shown in Figure 13 for an A_f of 0.007. The most obvious implication from this is that it enables the extension of the relaxation modulus results back a further three and one-half decades of shifted time.

CONCLUSIONS

The basic mechanical properties and constituent behavior of this developmental GAP/PSAN solid propellant are promising. An analysis of the maximum stress (strength) and the strain at maximum stress showed that there is a limited range of temperatures for any given strain rate where the measured strain at maximum stress exceeded 17%. The results suggest that the long-term equilibrium strain capability of this GAP/PSAN is between 10% and 12%.

The trend of the strength and tensile moduli were log-linear with the reciprocal of the strain rate across three decades. However, the shifted master curves were log-curvilinear in form. It was observed that the modulus versus the reciprocal of the strain rate data was characterized by two distinct trends in log space: at temperatures of −30°C and below, the slope of the curve was notably higher. The most probable reason for this is the reduction in the molecular mo-

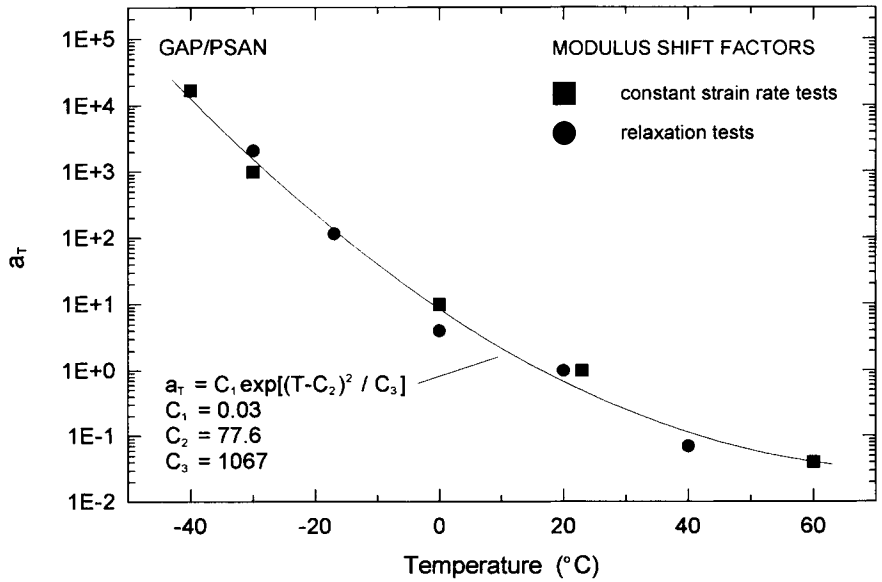

Figure 11 A comparison of the shift factors for the constant strain rate tensile modulus and the relaxation modulus.

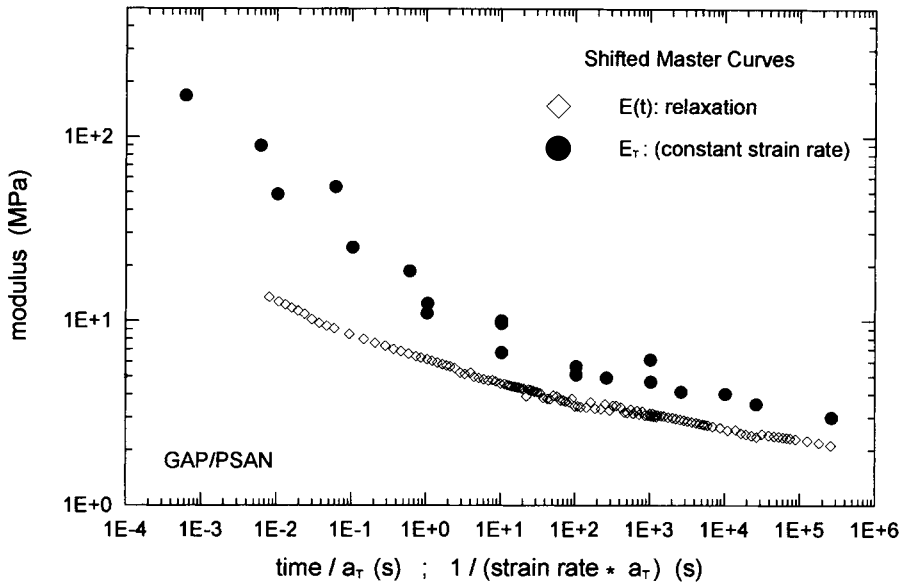

Figure 12 A comparison of the master modulus relaxation data and the master tensile modulus data from constant strain rate tests.

bility of the glycidyl azide polymer chains as the glass transition temperature is approached. A change in slope was also noted for the strength data, however it was restricted in occurrence to the data at −40°C, suggesting that more rigid, brittle-like behavior begins to affect the tensile modulus at higher temperatures than the strength.

A comparison between the shifted master modulus relaxation data obtained from relaxation tests and the shifted master tensile modulus data obtained from constant strain rate tests showed that the tensile moduli are consistently higher in value than the relaxation moduli for an equivalent shifted time. Where the two master curves overlap in time they show a similar trend and slope. Preliminary evidence suggests that the tensile modulus as a function of the reciprocal of shifted strain rate can be equated to the relaxation modulus as a function of shifted

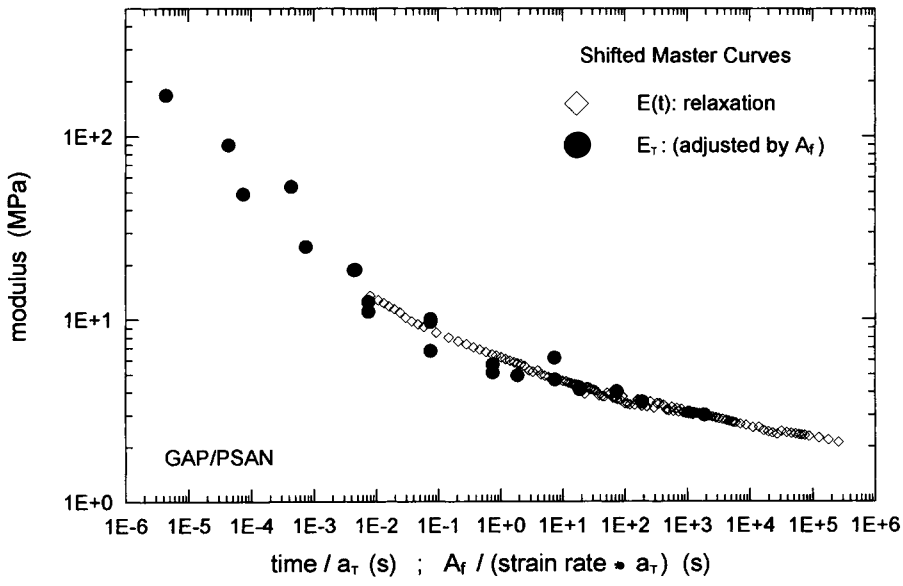

Figure 13 The master tensile modulus data from constant strain rate tests equated to the master modulus relaxation data through the adjustment factor A_f = 0.007.

time through an adjustment factor. This relationship extends the relaxation modulus results back a further three and one-half decades of shifted time.

The author thanks Mr. M. Kervarec for the preparation of the uniaxial test specimens and for his assistance in setting up the equipment to complete the experiments.

REFERENCES

1. P. Lessard, L. Druet, S. Villeneuve, S. Thiboutot, M. Benchabane, and D. Alexander, *Advisory Group for Aerospace Research and Development (NATO) Conf. Proc.*, **511,** 12-1 (1992).
2. *Chemical Propulsion Information Agency Publication 21,* The John Hopkins University Applied Physics Laboratory, Silver Spring, Md., November, 1970.
3. T. L. Smith, *J. Polym. Sci.,* **1,** 3597 (1963).
4. F. N. Kelley, *Appl. Polym. Symp.,* **1,** 229 (1965).
5. F. N. Kelley, in *Propellants Manufacture, Hazards and Testing,* C. Boyers and K. Klager, Eds., American Chemical Society, Washington, D.C., 1969, p. 188.
6. J. D. Ferry, *Viscoelastic Properties of Polymers,* Third Edition, John Wiley and Sons, Inc., New York, 1980.
7. R. G. Stacer, C. Hübner, and D. M. Husband, *Rubber. Chem. Technol.,* **63,** 488 (1990).
8. R. G. Stacer and D. M. Husband, *Rheol. Acta* **29,** 152 (1990).

Received July 31, 1994
Accepted October 1, 1994